Equilibrium of Field-Reversed Configuration Plasma Sustained by Rotating Magnetic Field

Kiyoyuki YAMBE, Michiaki INOMOTO[1)] and Shigefumi OKADA

Center for Atomic and Molecular Technologies, Osaka University, Osaka 565-0871, Japan

[1)]Graduate School of Frontier Sciences, The University of Tokyo, Chiba 277-8561, Japan

(Received: 1 September 2008 / Accepted: 2 December 2008)

We have measured detailed radial profiles of electron density and electron temperature in the field-reversed configuration (FRC) sustained by the rotating magnetic field (RMF). To study the influence on the equilibrium of two kinds of bias magnetic field configuration - straight (purely solenoidal) and mirror -, experiments have been carried out in the FRC Injection Experiment apparatus with metal vacuum vessel. The electron thermal pressure is well expressed as a function of magnetic flux during quasi-steady state in both configurations. In the straight bias field configuration, electron density increased with time only around the magnetic axis. On the other hand, in the mirror configuration, electron density increased with time in the entire plasma region. This is most appropriately ascribed to the improvement of confinement by strong mirror field of maximum mirror ratio of 4.0.

Keywords: field-reversed configuration, rotating magnetic field, equilibrium, mirror field

1. Introduction

Field-reversed configuration (FRC) is a compact torus plasma which is sustained solely by a poloidal magnetic field and thus has extremely high-β value [1]. FRCs have traditionally been formed by field-reversed theta-pinch's (FRTP's) [2] and plasma merging [3]. In these cases, the plasma decayed in less than 1 ms and quasi-steady sate was not long enough to accomplish measurement required for detailed discussion on equilibrium. Recently, quasi-stationary FRC is achieved by the transverse rotating magnetic field (RMF) [4-12]. The lifetime of the FRC sustained by the RMF (RMF-FRC) is longer than 1 ms and quasi-steady state becomes long accordingly. In addition, the RMF-FRC has low density and temperature compared with the FRC plasma produced by the FRTP and the plasma merging. It is suited for detailed spatiotemporal measurement by electrostatic probes.

In this study, we have measured detailed radial profiles of electron density and electron temperature in the FRC sustained by the RMF. We will show a comparison of radial profiles of FRC plasmas sustained in straight bias magnetic field and mirror bias magnetic field.

2. Apparatus

Experiments have been carried out in the confinement section of the FRC Injection Experiment (FIX) apparatus [9-12]. The vacuum vessel is made of stainless-steel whose length is 3.4 m and inner radius is 0.4 m. Figure 1 shows the schematic view of the confinement section of the FIX apparatus. Figure 2 shows the cross-sectional view of the FIX apparatus at z = 0 mm. The bias magnetic field

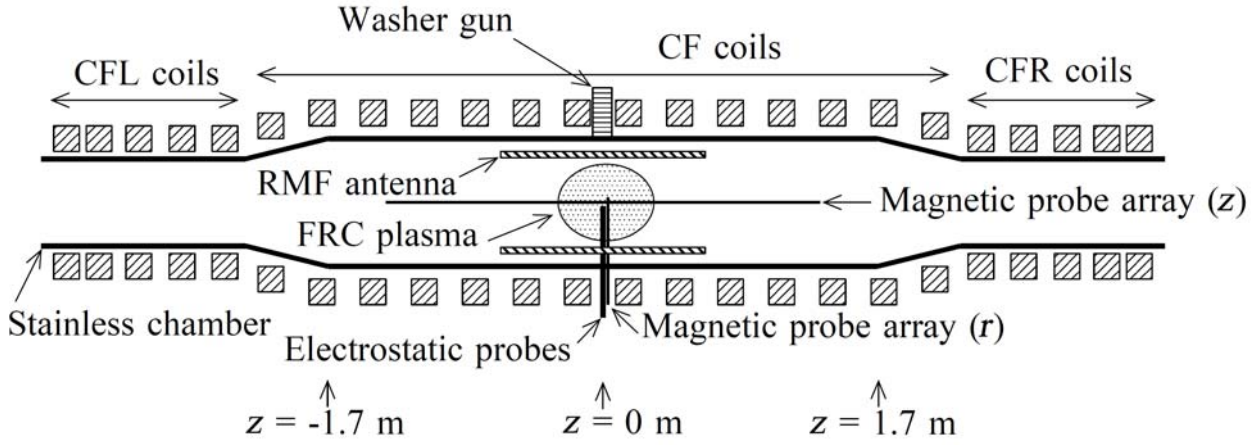

Fig. 1. Schematic view of the confinement section of the FIX apparatus.

Author's e-mail: k-yambe@ppl.eng.osaka-u.ac.jp

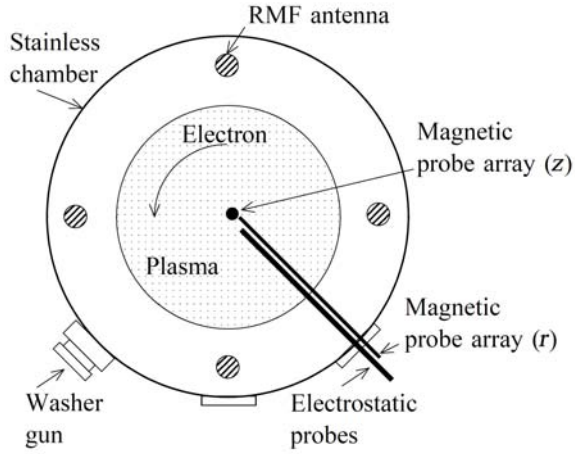

Fig. 2. Cross-sectional view on the mid-plane of the FIX apparatus.

is about 5 G at the center axial position of z and r = 0 mm. Straight bias magnetic field is generated by the CF coils. Mirror bias magnetic field is generated by the CFL+CFR coils. Figure 3 shows the axial profiles of axially bias magnetic field B_z in straight and mirror bias magnetic fields. The transverse rotating magnetic fields are generated by two pairs of RMF antennas located at r = 330 mm and from z = - 600 to 600 mm. The maximum value of the RMF current I_{RMF} is about 800 A and it decreases gradually due to the limitation of power supply system in the latter half of the discharge. The RMF frequency is 106 kHz, which is higher than the ion-cyclotron frequency (~ 7.6 kHz). The RMF-FRC in the FIX has RMF with high spatial harmonics due to the conducting vacuum vessel [10]. The excluded high-harmonic components generate effective magnetic field pressure near the plasma edge, which helps to keep the separatrix away from the vessel wall. A pre-ionized hydrogen gas is supplied by a washer gun.

The measurement system is composed of an axial and radial magnetic probe arrays and electrostatic probes. The radial magnetic probe array measures the radial profile of an axial magnetic field B_z at the azimuthal location of 45 degree away from the RMF antenna. The electrostatic probes measure electron density n_e and electron temperature T_e at the same azimuthal location as the radial magnetic probe array. The n_e and T_e are calculated by the triple-probe current method [13]. The signals are digitized and the noise due to the RMF is removed by using a digital low-pass filter with a cut-off frequency of 150 kHz.

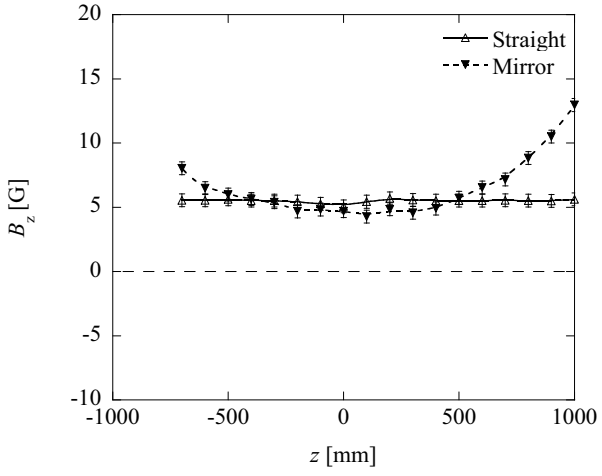

Fig. 3. Axial profiles of axial magnetic field B_z at vacuum in straight and mirror configurations of bias magnetic field.

3. Experimental Results

Typical time evolutions of I_{RMF}, B_z, and n_e in two different bias magnetic field configurations - straight (purely solenoidal) and mirror - are shown in Fig. 4. The RMF power is supplied from t = 0.4 to 3.2 ms. The absolute value of RMF current keeps constant value of about 750 A from 0.5 to 1.5 ms. The RMF current starts to decrease by about 5 % from 1.5 to 2.0 ms and by about 30 % from 2.0 to 3.0 ms. The field-reversal in the straight configuration starts to decrease by about 30 % from 1.0 to 2.0 ms and about 70 % from 2.0 to 2.4 ms. The field-reversal disappears at t ~ 2.4 ms even when the RMF is supplied. In the mirror configuration, on the other hand, field-reversal is maintained at almost constant level from 0.8 to 2.6 ms regardless of slight decay in RMF current

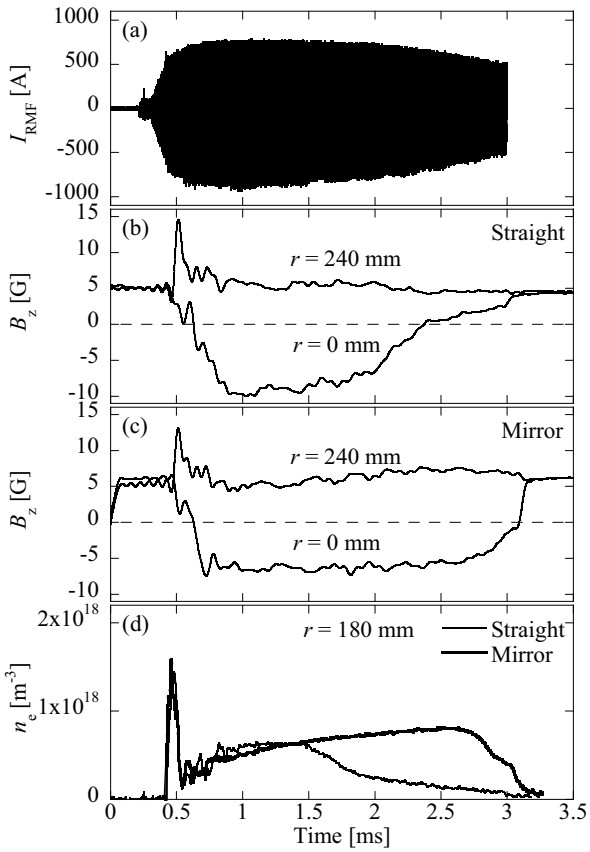

Fig. 4. Time evolutions of (a) RMF current I_{RMF}, (b) B_z in straight configuration, (c) B_z in mirror configuration, and (d) electron density n_e.

and it starts to decrease from $t \sim 2.6$ ms when the I_{RMF} decreased by about 20 %. The electron density in the straight configuration starts to decrease at $t \sim 1.5$ ms prior to the start of decay of field-reversal. In the mirror configuration, the electron density increases until $t \sim 2.6$ ms and then starts to decrease just as the field-reversal starts to decrease. Quasi-steady state is from $t = 0.9$ to 1.5 ms in the straight configuration and in the mirror configuration, it is from $t = 0.8$ to 2.6 ms.

The radial profiles of B_z, magnetic flux Ψ, and electron thermal pressure $n_e kT_e$ at $t = 1.4$ ms are shown in Fig. 5. The data of each discharge is averaged between 1.35 and 1.45 ms over five discharges. The radius of the magnetic null R is about $R \sim 180$ mm, or Ψ is the deepest here in both the straight and the mirror configurations. The separatrix radius r_s is determined to be about 260 mm from the radial profile of Ψ. The electron density near the separatrix is almost the same as that at the center geometrical axis in both the straight and the mirror configurations. The radial profile of $n_e kT_e$ depends only on the electron density profile because the electron temperature is almost uniform [12]. Therefore, in both the straight and the mirror configurations, $n_e kT_e$ at the geometric axis is almost equal to that near the separatrix.

The dependences of $n_e kT_e$ on Ψ/Ψ_{max} at $t = 1.4$ ms in the straight and mirror configurations are shown in Fig. 6. The electron thermal pressure on the inner flux surfaces is almost equal to that on the corresponding outer flux surfaces in both the straight and the mirror configurations. Electron thermal pressure is well expressed as a function of Ψ in both the straight and the mirror configurations. Discrepancy at $\Psi/\Psi_{max} = 0$ may be ascribed to the error of

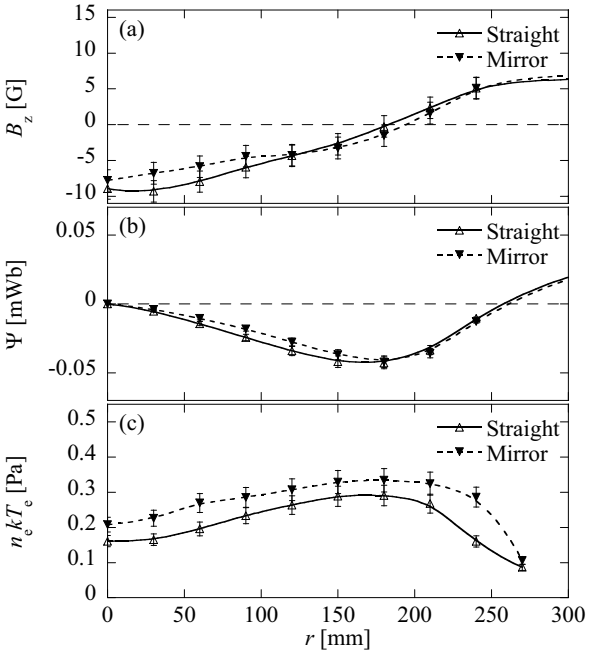

Fig. 5. Radial profiles of (a) B_z, (b) magnetic flux Ψ, and (c) electron thermal pressure $n_e kT_e$ at $t = 1.4$ ms in straight and mirror configurations.

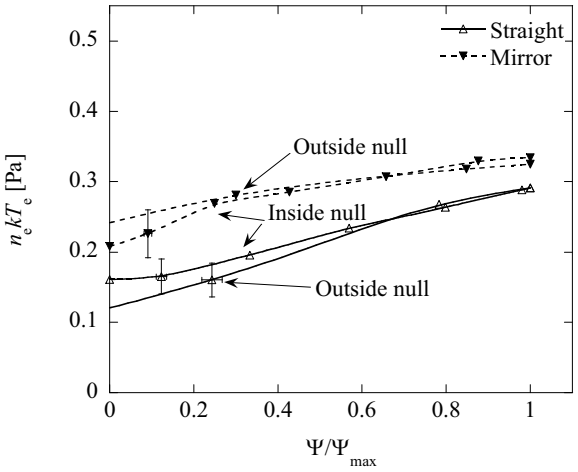

Fig. 6. Dependences of $n_e kT_e$ on Ψ/Ψ_{max} at $t = 1.4$ ms in straight and mirror configurations.

measurement because both Ψ and $n_e kT_e$ changes rapidly at $r = r_s$. Even if functional from of $p(\Psi)$ changes with time, p continues to be expressed by Ψ during the quasi-steady state in both the straight and the mirror configurations.

The axial profiles of the axial magnetic field B_z at $t = 1.4$ ms in the straight and the mirror configurations are shown in Fig. 7. The separatrix length is almost same in both configurations. In the straight configuration, the axial magnetic field outside the plasma $|z| > 700$ mm is about 5 G. In this case, a mirror ratio r_M in the open field region is about 0.71 at $z = 1700$ mm. On the other hand, in the mirror configuration, the axial magnetic field continues to increase in the outside region of the plasma. The value of r_M is about 4.0 at $z = 1700$ mm.

In the mirror configuration, the lifetime of field-reversal is maintained as far as the RMF power is supplied. Time evolutions of radial profile of electron density in the straight and the mirror configurations are shown in Figs. 8(a) and 8(b), respectively. In the figures, each data is evaluated for the 0.1 ms time durations (ex.

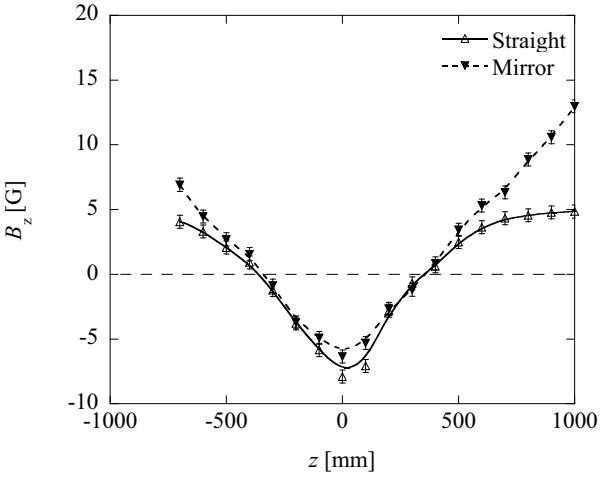

Fig. 7. Axial profiles of B_z at $t = 1.4$ ms in straight and mirror configurations.

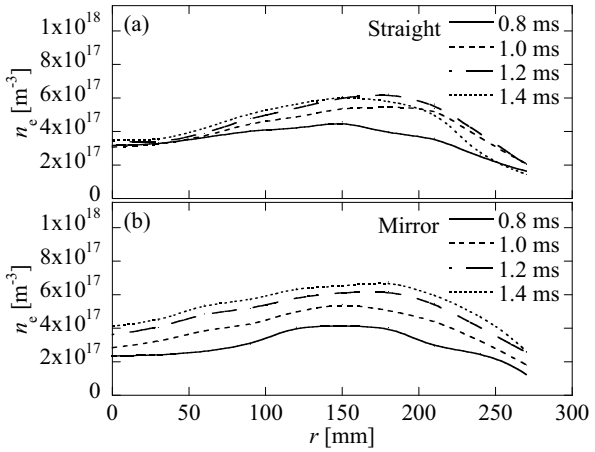

Fig. 8. Radial profiles of n_e in (a) straight and (b) mirror configurations of bias magnetic field.

1.0 ms indicates between 0.95 and 1.05 ms interval). In the straight configuration, the electron density increases only near the magnetic null point. In the mirror configuration, the electron density increases in the entire radial location. The tendency that the electron density at the separatrix is almost equal to that at the center does not change even if the density increases.

4. Discussion

The tendency for the density build up is seen in both straight and mirror configurations. This will be explained by the fact that the density of neutral particle n_n is estimated to be $n_n < 5 \times 10^{17}$ m^{-3} [11]. For $n_n = 5 \times 10^{17}$ m^{-3}, $n_i = 5 \times 10^{17}$ m^{-3}, and $T_i = 3$ eV, ionization time is estimated to be about 0.1 ms [14]. In more detail, in the straight field configuration, the density builds up only around the magnetic axis. On the other hand, in the mirror configuration, the density build up is observed in the entire region. Considering the fact that the mean free path of the electron is about 2.3 m, these observation will be explained from the consideration on the confinement.

Spatial region accessible by a particle with given (H, P_θ) (here H; Hamiltonian, P_θ; canonical momentum) is either closed or open [15]. The particle which constitutes former region (open Stoermer region) is confined and the region tends to be more inside the plasma surrounding the magnetic axis. On the other hand, the latter region (closed Stoermer region) tends to be outside of the former one and it extends out of the confinement chamber through the region with mirror field. From these fact, in the straight bias field configuration, particle confinement around the magnetic axis will be lower than the region near the separatrix and the observed behavior that the density builds up only around the magnetic axis will be explained. In addition, in the mirror configuration, particle confinement will be improved by the mirror field, which will cause the observed increase of density in the entire plasma region.

5. Summary

Detailed magnetic and electrostatic probes measurement has been carried out to investigate the influence of the straight and the mirror configurations of bias magnetic field. In the straight bias configuration, field-reversal disappears even when the RMF is supplied. In the mirror bias configuration, on the other hand, the field-reversal is maintained as far as the RMF power is supplied. The electron thermal pressure is well expressed as a function of Ψ during quasi-steady state in both the straight and the mirror bias configurations. In the mirror bias configuration different from the straight bias configuration, electron density builds up over entire plasma region, which behavior is explained by the improved confinement in the open Stoermer region brought about by the mirror field.

References

[1] M. Tuszewski, Nucl. Fusion **28**, 2033 (1988).
[2] W. T. Armstrong *et al*., Phys. Fluids **24**, 2068 (1981).
[3] Y. Ono and M. Inomoto, Phys. Plasmas **7**, 1863 (2000).
[4] I. R. Jones, Phys. Plasmas **6**, 1950 (1999).
[5] W. N. Hugrass, Plasma Phys. Control. Fusion **42**, 1219 (2000).
[6] J. T. Slough and K. E. Miller, Phys. Plasma **7**, 1945 (2000).
[7] H. Y. Guo *et al*., Phys. Plasmas **9**, 185 (2002).
[8] A. L. Hoffman *et al*., Nucl. Fusion **45**, 176 (2005).
[9] S. Okada *et al*., Nucl. Fusion **45**, 1094 (2005).
[10] M. Inomoto *et al*., Phys. Rev. Lett. **99**, 175003 (2007).
[11] M. Inomoto *et al*., Plasma Fusion Res. **3**, 004 (2008).
[12] K. Yambe *et al*., Phys. Plasmas **15**, 092508 (2008).
[13] S. -L. Chen and T. Sekiguchi, J. Appl. Phys. **36**, 2363 (1965).
[14] R. J. Goldston and P. H. Rutherford, *Introduction to Plasma Physics* (Institute of Physics Publishing, London, 1995) p.155.
[15] M. -Y. Hsiao and G. H. Miley, Nucl. Fusion **24**, 1029 (1984).